

Protostellar collapse: rotation and disk formation

W. M. Tscharnuter¹, J. Schönke¹, H.-P. Gail¹, M. Tieloff², and E. Lüttjohann¹

¹ Zentrum für Astronomie (ZAH), Institut für Theoretische Astrophysik (ITA), Universität Heidelberg, Albert-Ueberle-Str. 2, 69120 Heidelberg, Germany
e-mail: wmt@ita.uni-heidelberg.de

² Institut für Geowissenschaften, Universität Heidelberg, Im Neuenheimer Feld 236, 69120 Heidelberg, Germany

Received 20 March 2009 / Accepted 8 June 2009

ABSTRACT

We present some important conclusions from models of the collapse of rotating molecular cloud cores with axial symmetry, corresponding to the evolution of young stellar objects from class 0 to the beginning of class I. There are three main findings of the calculations: (1) the typical timescale for building up a preplanetary disk, which was found to be of the order of one free-fall time decisively shorter than the widely assumed timescale related to the so-called “inside-out collapse”; (2) redistribution of angular momentum and the accompanying dissipation of kinetic (rotational) energy causing the growing disk to become more stable and strengthening the intrinsic meridional circulation pattern of the accretion flow; and (3) the origin of calcium-aluminium-rich inclusions (CAIs). Because of the persistent equatorial outflow, material that has undergone substantial chemical and mineralogical modifications in the hot (≥ 900 K) interior of the protostellar core may have a good chance of being advectively transported outward into the cooler remote parts (≥ 4 AU, say) of the growing disk and surviving there until it is incorporated into a meteoritic parent body.

Key words. stars: formation – accretion, accretion disks – planetary systems: formation

1. Introduction

Stars are understood to form from regions within molecular clouds that for some reason became gravitationally unstable and started to collapse under the influence of their own gravitational attraction (see, e.g., Larson 2003; McKee & Ostriker 2007). It is clear that angular momentum (e.g., Bodenheimer 1995; Tohline 2002) and magnetic fields (e.g., Pudritz et al. 2008) play an important role during many stages of protostellar collapse. Angular momentum is particularly important because it is responsible for the formation of accretion disks that are the birthplaces of planetary systems. Therefore, the study of rotating collapse is inevitable if one intends to understand the formation of the Solar System and other planetary systems.

The earliest of such studies were a number of analytic approaches to rotating collapse without (Terebey et al. 1984) and with (Allen et al. 2003) magnetic fields and analytic studies of disk formation (see Cassen 1994, and references therein) and simple models for the build-up and evolution of accretion disks (e.g., Lin & Pringle 1990; Nakamoto & Nakagawa 1994). These introduce a number of approximations about the nature of the collapse process that appear plausible but lack justification.

In the past two decades, various attempts have been made to follow the 2-D and 3-D collapse of rotating protostellar fragments by means of extended numerical calculations (e.g., Boss 1989; Bodenheimer et al. 1990; Yorke et al. 1993; Saigo et al. 2008) based on grid-methods, by a solution method based on a series development into orthogonal polynomials (Tscharnuter 1987), and by studies based on the SPH-method (e.g., Stamatellos et al. 2007).

However, almost all of these studies covered only the collapse up to the formation of the first core. Only the early 2-D model of Tscharnuter (1987), the 3-D study of Bate (1998) and the models of Stamatellos et al. (2007) and Saigo et al. (2008)

achieved sufficient resolution to follow the second collapse. As a rule, 3-D models neglect most of the basic physics and consider only an oversimplified equation of state. Promising ideas to overcome this unfortunate situation have been put forward by Stamatellos et al. (2007).

In this paper, we discuss some important cosmochemical consequences of a new 2-D model calculation by following simultaneously the evolution of a rotating Bonnor-Ebert-sphere-like initial state with $\sim 1 M_{\odot}$ initial mass through an axially-symmetric first and second collapse to nearly stellar central densities and the early build-up and evolution of the associated accretion disk. The model takes all of the essential physics of the problem into account and the simulation covers the evolutionary phases of young stellar objects corresponding to class 0 and early class I. It clearly demonstrates the rapid co-formation of a compact stellar object and a very extended accretion disk within a period of no more than ~ 1.1 free-fall times.

2. Methods

Appropriate implicit methods have been developed only for 1-D and 2-D collapse problems with spherical and axial symmetry, respectively (see, e.g., Wuchterl & Tscharnuter 2003; Tscharnuter 1987). Of course, implicit methods (being notoriously expensive) are useful only if the physical processes to be considered exhibit a hierarchy of timescales and the system as a whole evolves into a quasi-stationary state. If the longest timescale exceeds the smallest one by a large amount, the use of implicit methods is mandatory, as in our case, where the accretion time is several orders of magnitude longer than the oscillation period of the stellar core.

For a detailed description of the method upon which the implicit 2-D hydrodynamical code is based, we refer to Tscharnuter (1987). For the equation of state, both the dissociation of H_2 and

Table 1. Starting parameters.

Quantity	Symbol	Value	Dimension
mass	M	1.037	M_{\odot}
angular momentum	L	2.682×10^{53}	$\text{g cm}^2 \text{s}^{-1}$
radius	R	1.200×10^{17}	cm
spin angul. veloc.	Ω	3.160×10^{-14}	s^{-1}
centrifugal barrier	R_{cfb}	1.504×10^{15}	cm
mean density	$\bar{\rho}$	2.850×10^{-19}	g cm^{-3}
mean free-fall time	$\bar{t}_{\text{ff}} = \sqrt{\frac{3\pi}{32G\bar{\rho}}}$	1.247×10^5	yr
central density	ρ_c	5.326×10^{-18}	g cm^{-3}
central free-fall time	$t_{\text{ff,c}} = \sqrt{\frac{3\pi}{32G\rho_c}}$	2.885×10^4	yr
temperature	T	10	K
ratio rot./grav. energy	$\theta = \frac{E_{\text{rot}}}{ E_{\text{grav}} }$	2.437×10^{-3}	–

ionization of H and He is taken into account, and the opacities at low temperatures are dominated by dust with and without ice mantles. In a spherical polar coordinate system, we discretize the variables within a staggered radial grid (256 gridpoints) and represent the dependence on the polar angle by choosing a Legendre expansion (up to 27 coefficients) for each primary variable. The discretized equations are written in a conservation form on a self-adaptive radial grid according to [Dorfi & Drury \(1987\)](#), and the shock fronts are smoothed by artificial (tensor-) viscosity. The maximum resolution achieved amounts to about $0.03 R_{\odot}$ in the central parts. The adaptive grid is chosen in a way that the innermost rigidly rotating homogeneous sphere always contains a fraction of 10^{-6} of the total mass.

Concerning the coefficient of turbulent viscosity, ν_{tur} , we have adopted the so-called β -viscosity prescription of [Duschl et al. \(2000\)](#), an extension of the well-known, but likewise heuristic, α -viscosity for application to self-gravitating disks. To be specific, $\nu_{\text{tur}} := \beta r^2 \Omega$, where r is the radial coordinate, Ω the (local) angular velocity, and $\beta = 10^{-4} \dots 10^{-2}$ the inverse of the critical Reynolds number indicating the onset of turbulence. In our calculation, we have chosen $\beta = 10^{-2}$.

3. Results and conclusions

3.1. Initial configuration and the first collapse phase

Table 1 lists a set of appropriate starting parameters leading to the collapse of a rotating protostellar cloud fragment. The Bonnor-Ebert-sphere-like initial configuration exhibits already a moderate density concentration toward the center and is assumed to rotate like a rigid body. The revolution period, $2\pi/\Omega = 6.3 \times 10^6$ yr, adopted in our calculation is long compared to the mean free-fall time. Hence, the centrifugal barrier is situated at a distance from the center of only about 1% of the cloud radius, and the collapse flow develops almost perfectly with spherical symmetry for most parts of the cloud.

It is convenient to reset the clock to zero when the optical depth of the collapsing fragment, counted from the outer edge to the center, exceeds $2/3$ for the first time (e.g., [Wuchterl & Tscharnuter 2003](#)). This event may be interpreted to be the beginning of the protostellar evolution. All ages given subsequently are relative to this moment.

Shortly after age zero, an accretion shock forms marking the natural boundary of a flattened quasi-hydrostatic rotating structure, which is pressure-supported, parallel, and centrifugally-supported perpendicular to the axis of rotation.

3.2. Formation and growth of the disk-like core

Figure 2 shows (a) the density-temperature-diagram for the very center of the collapsing cloud, (b) the stability parameter θ_c as a function of the relative core mass M_c/M_{tot} , and (c) the time dependence of the relative core mass. The labels A through E indicate characteristic stages of the evolution:

- A: the core starts to grow in mass;
- B: continuation of the accretion after thermal relaxation caused by opacity effects (sublimation of ice mantles);
- C: sublimation of the dust grains commences off-center near the axis of rotation as a “hot polar cap”, leaving a growing opacity gap and violent thermal relaxation effects;
- D: start of the second collapse due to dissociation of H_2 ;
- E: formation of the “stellar” core.

Our first important result is that we found a typical rise time, M_c/\dot{M}_c , of the core’s mass to be only a small fraction (1–2%) of the mean free-fall time, i.e., only a few thousand years. Figure 2c shows an almost constant accretion rate of $3 \times 10^{-5} M_{\odot} \text{yr}^{-1}$ lasting for about 2600 yr, from slightly after “A” until “D”, where the second collapse sets in. The dots between “D” and “E” represent the individual models tracing the dynamical transition (the “second collapse”) from the disk-forming first core to the second “stellar” core.

Figure 1 demonstrates the increasing geometrical dimensions and the changing shape of the first core, which occurs within a few thousand years; the bulge in the polar direction, indicated by the route of the accretion shock in the vicinity of the rotational axis, is the result of a rather intricate interplay between the redistribution of angular momentum, the accompanying generation of entropy (viz. heat), and the transport of energy. The net effects are rising temperatures and lower rotation rates in the inner parts of the core, which are necessary to trigger the second collapse. Test calculations demonstrated that, without a certain amount of angular momentum transport, the core would stay too cool and, hence, become prone to the onset of destructive gravitational instabilities that trigger binary formation.

A glimpse at Fig. 2b indicates that the first core cannot escape from existing in the regime of secular instability. The ratio, $\theta = E_{\text{rot}}/|E_{\text{grav}}|$ ¹, quickly rises above the critical number of 0.14, so that a small amount of dissipation leads to symmetry breaking: the originally axisymmetric core will assume a triaxial shape and presumably evolve into a distinctive bar/spiral configuration exerting gravitational torques, which, in turn, cause an enhanced redistribution of angular momentum (see, e.g., [Bodenheimer & Ostriker 1973](#); [Ostriker & Bodenheimer 1973](#); [Pickett et al. 1997](#); [Toman et al. 1998](#); [Imamura et al. 2000](#)). This finding may motivate our choice of rather efficient turbulent (β -) viscosity with $\beta = 0.01$.

3.3. Formation of the “stellar” core

The second collapse is a result of the interplay between thermodynamics, redistribution of angular momentum as a dissipative process, and energy transport. Their combined effect is illustrated by Fig. 1: particularly in the central parts, angular momentum transport tends to prevent extreme flattening, while the heat input by the accompanying dissipation of rotational energy creates increasing pressure forces. As a consequence, the pressure distribution becomes more spherical, and after some “incubation” period of slow contraction (between “C” and “D” in

¹ Usually written $\beta := T/|W|$, but we wish to avoid confusion with T , the temperature, and β , the scaling parameter of the turbulent viscosity.

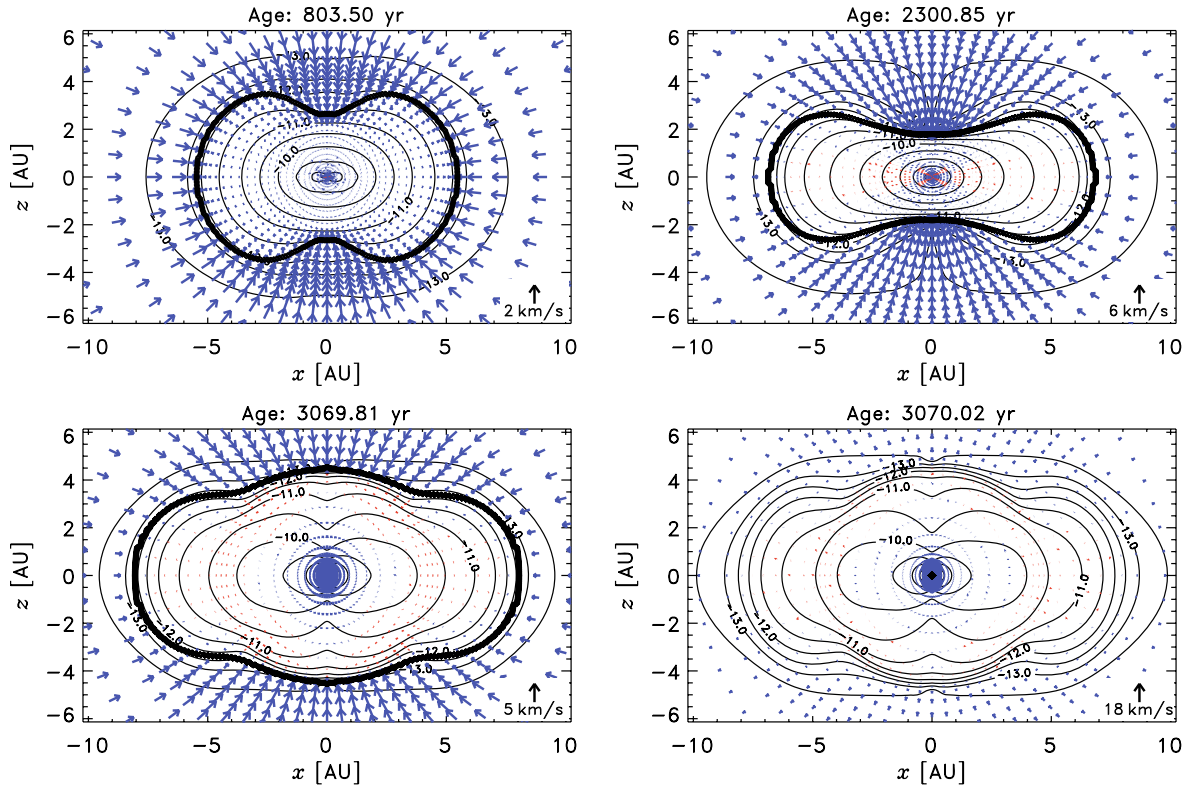


Fig. 1. Meridional cross sections. Displayed are equi-density contours (annotated numbers are logarithms of the density in g cm^{-3}), the spacing being 0.5 dex, and arrows representing the velocity field. Red “spots” indicate expansion (cf. Fig. 3a). The closed heavy line marks the accretion shock, and the arrow at the lower right corner of the four panels represents the respective maximum infall velocities. *Upper row:* snapshots slightly after B and before C, respectively. *Lower row:* snapshots for D and E (cf. Fig. 2). At E (*right panel*), two shocks, an outer and an inner one, bounding the growing “pre-planetary” disk and the “stellar” core, respectively, coexist (the two shocks are not displayed here, but cf. Fig. 4 for the formation of the stellar core).

Fig. 2), dissociation of H_2 eventually leads to dynamical collapse (“D”–“E”). Figure 2b shows that the stability parameter, θ_c , approaches the critical value of 0.27, which is indicative of dynamical instability. Interestingly enough, our axisymmetric model suggests the formation of a self-gravitating doughnut-like structure of the density distribution (cf. Fig. 4).

3.4. An intermediate hot solar nebula?

The model provides for the first time a realistic initial temperature and density structure of the accretion disk and the flow pattern in the disk and its surroundings, including well resolved accretion shocks, on scales as small as well below 1 AU. Figure 3b shows a rather hot inner disk region extending out to about 4 AU. This structure was not seen in earlier calculations because of a lack of resolution, use of inadequate equations of state, and the omission of radiative transfer; it lasts for a couple of 1000 yr. This inner portion is hot enough for formation of materials such as those found as calcium-aluminium rich inclusions (CAIs) in meteorites; it might be the “hot solar nebula” that cosmochemists have always advocated.

CAIs are a fundamental – though rare (few permille to percent) – ingredient of chondrites. Although modified by a secondary processing, they consist of mineral assemblages which are expected for high temperature (>1600 K) solar nebula condensates, and are considered to be oldest solar system material (Amelin et al. 2002; Bouvier et al. 2007) and apparently formed over a relatively short time interval, but their detailed formation setting is basically unknown.

The CAI formation time interval has been vividly debated, based on short-lived nuclide chronometry, mainly the ^{26}Al – ^{26}Mg system ($\tau_{1/2} = 0.7$ Ma). While most studies yielded a so-called “canonical” initial $^{26}\text{Al}/^{27}\text{Al}$ in the range 5×10^{-5} , Thrane et al. (2006), Young et al. (2005), and Bizzarro et al. (2004) argued for a “supracanonical” $^{26}\text{Al}/^{27}\text{Al}$ ratio of $5.8 \dots 7 \times 10^{-5}$, implying formation and processing of CAI material over a few 100 000 years. Jacobsen et al. (2008) expended a comprehensive effort to demonstrate that CAIs have an identical (canonical) $^{26}\text{Al}/^{27}\text{Al}$ ratio of $5.23 \pm 0.13 \times 10^{-5}$, implying a formation time interval of only 40 ka.

After residence in the solar nebula the CAIs became incorporated into chondritic parent bodies, which are strongly related to carbonaceous chondrites. This must have happened up to a few Ma later, as indicated by chondrule ages. Chondrules formed before chondrite parent-body accretion and are 1–4 Ma younger than CAIs (e.g., Scott 2007). It has always been unclear how they could be dynamically transported from their apparent formation regions in the inner solar system outwards to chondrite forming regions, and survive a few Ma before becoming incorporated into carbonaceous chondrite parent bodies. Our model shows that from the onset of disk formation on, there is a complex accretion flow structure, where the average inflow is superimposed on circulation currents that result in a net outward directed flow close to the midplane and inward directed flow in higher layers of the disk (cf. Fig. 1). This flow results in both accretion and a large-scale transport of matter (with velocities $10\text{--}50 \text{ m s}^{-1}$, cf. Fig. 3a) close to the disk’s midplane from the hot part outward to distances of several AU from the center.

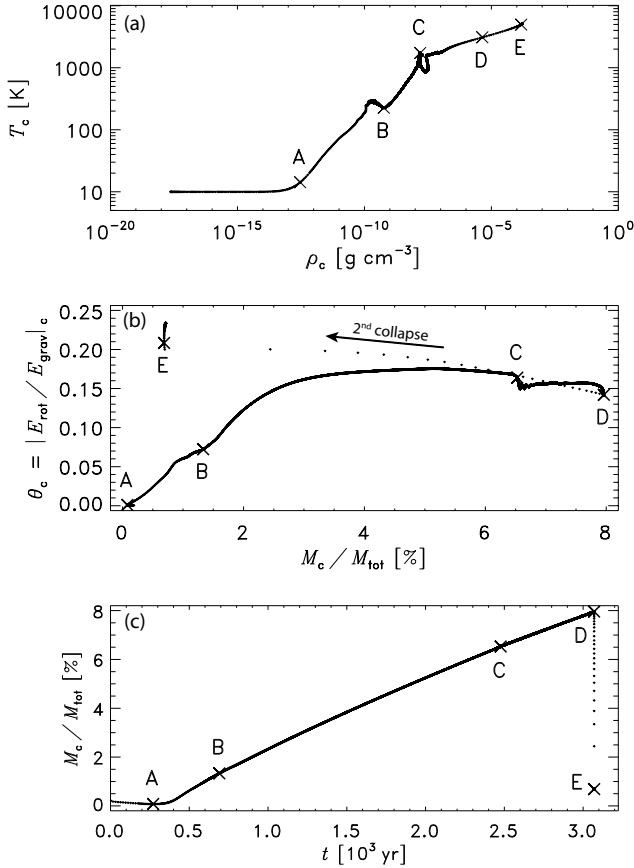


Fig. 2. Evolution of the core. **a)** central density vs. central temperature; **b)** ratio of rotational over gravitational energy vs. core mass; **c)** core mass vs. time. Plotted are the respective quantities for each of the 10^4 timesteps individually. Because of the rapid evolution during the second collapse the path from D to E is covered only by a few points. For the meaning of labels A through E see Sect. 3.2.

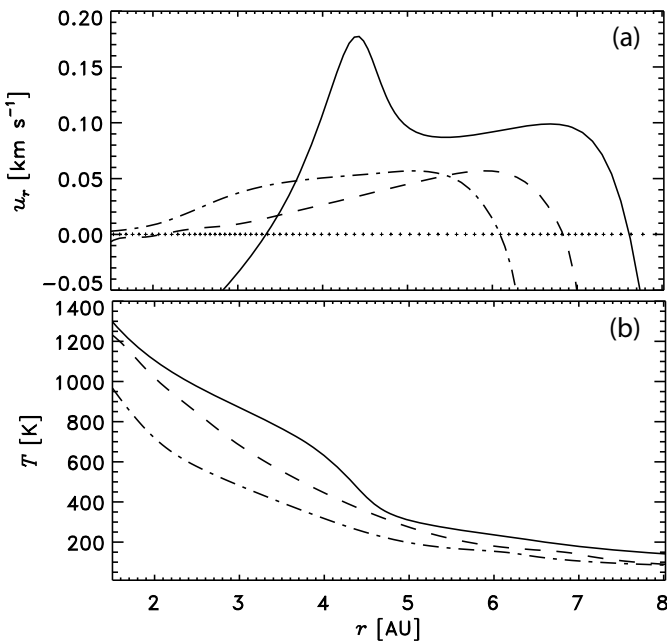


Fig. 3. Evolution of the core from its quasi-stationary stage to the end of the second collapse. Spatial distribution of **a)** the radial velocity component, u_r , **b)** the temperature, T , in the equatorial plane for three instants of time indicated by dash-dotted (2301 yr), dashed (2948 yr), and solid lines (3070 yr), respectively; crosses mark the gridpoints.

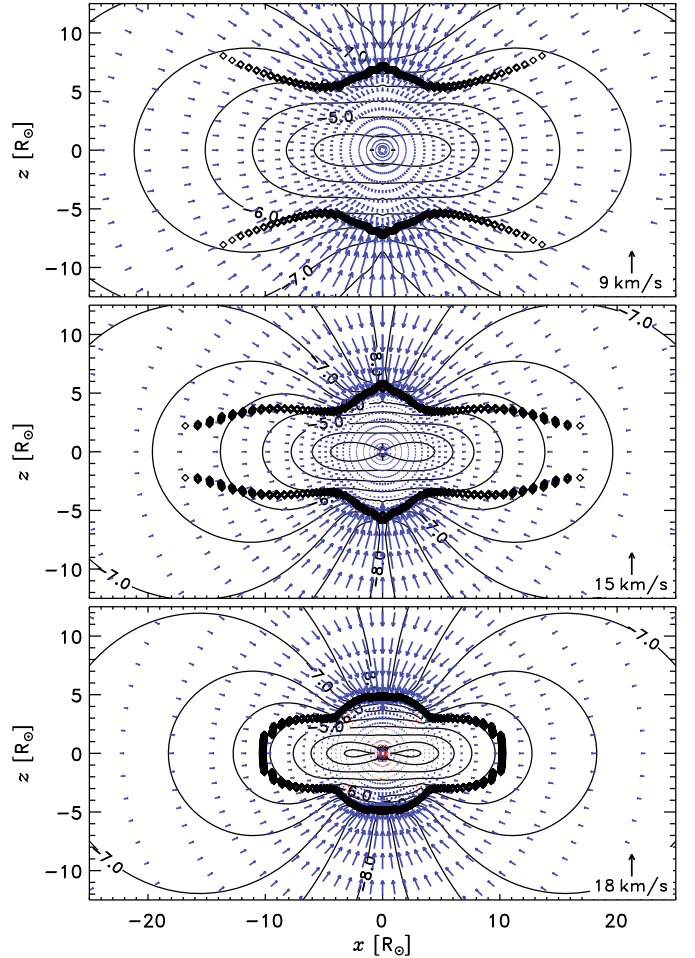


Fig. 4. Meridional cross sections (cf. Fig. 1). Formation of the “stellar” core on a very short timescale. Plotted are three snapshots of the final shock evolution at (from above) $t_0 - 10$ d, t_0 , and $t_0 + 7$ d, respectively, with $t_0 = 3070$ yr. The contour lines and arrows have the same meaning as in Fig. 1, numbers are again logarithms of the density in g cm^{-3} , the spacing is 0.5 dex, and the arrows indicate the velocity field. Note that now the geometrical dimensions are only several solar radii (R_\odot).

This type of global accretion flow structure is generally found in hydrodynamic calculations (e. g., Kley & Lin 1992; Różyczka et al. 1994; Keller & Gail 2004). Material from the hot region may be mixed by this across the inner ~ 5 AU and part of this material may survive until the onset of planetesimal formation since outflow close to the midplane also continues to exist in later phases of disk evolution, though with reduced velocity (e.g., Keller & Gail 2004; Ciesla 2009). In the full 3-D picture, the flow will presumably exhibit non-axisymmetric structures (e.g., cyclones). However, since they are only local phenomena, we do not expect them to impede the global meridional circulation considerably.

According to these perceptions, our model provides a most feasible setting for CAI formation comprising a very short time interval at the starting point of stellar accretion, which implies both high temperature processing out to relatively large inner disk radii, and a possible outward transport mechanism to ensure survival and later incorporation into chondritic planetesimals. Although other disk activities may also provide high temperature energetic events (e.g., FU Orionis outbursts), they were mostly active on significantly longer timescales, and appear

unsuitable to explain why CAIs formed over such a restricted time interval of 40 ka only.

The model therefore seems to offer an explanation of how the short CAI-forming period in the Solar Nebula is related to the earliest evolutionary phase of the accretion disk. If true, CAI formation follows the second collapse immediately and is an accurate indicator of the formation time of the protoplanetary disk.

Acknowledgements. This work has been supported by the Forschergruppe 759, “The Formation of Planets: The Critical First Growth Phase” of the Deutsche Forschungsgemeinschaft (DFG).

References

- Allen, A., Li, Z.-Y., & Shu, F. H. 2003, *ApJ*, 599, 363
 Amelin, Y., Krot, A. N., Hutcheon, I. D., et al. 2002, *Science*, 297, 1678
 Bate, M. R. 1998, *ApJ*, 508, L95
 Bizzarro, M., Baker, J. A., & Haack, H. 2004, *Nature*, 431, 275, Erratum: 2005, *Nature*, 435, 1280
 Bodenheimer, P. 1995, *ARA&A*, 33, 199
 Bodenheimer, P., & Ostriker, J. P. 1973, *ApJ*, 180, 159
 Bodenheimer, P., Yorke, H. W., Różyczka, M., et al. 1990, *ApJ*, 355, 651
 Boss, A. P. 1989, *ApJ*, 345, 554
 Bouvier, A., Blichert-Toft, J., Moynier, F., et al. 2007, *Geochim. Cosmochim. Acta*, 71, 1583
 Cassen, P. 1994, *Icarus*, 112, 405
 Ciesla, F. J. 2009, *Icarus*, 200, 655
 Dorfi, E. A., & Drury, L. O. 1987, *J. Comp. Phys.*, 69, 175
 Duschl, W. J., Strittmatter, P. A., & Biermann, P. L. 2000, *A&A*, 357, 1123
 Imamura, J. N., Durisen, R. H., & Pickett, B. K. 2000, *ApJ*, 528, 946
 Jacobsen, B., Yin, Q., Moynier, F., et al. 2008, *Earth Plan. Sci. Lett.*, 272, 353
 Keller, C., & Gail, H.-P. 2004, *A&A*, 415, 1177
 Kley, W., & Lin, D. N. C. 1992, *ApJ*, 397, 600
 Larson, R. B. 2003, *Reports on Progress in Physics*, 66, 1651
 Lin, D. N. C., & Pringle, J. E. 1990, *ApJ*, 358, 515
 McKee, C. F., & Ostriker, E. C. 2007, *ARA&A*, 45, 565
 Nakamoto, T., & Nakagawa, Y. 1994, *ApJ*, 421, 640
 Ostriker, J. P., & Bodenheimer, P. 1973, *ApJ*, 180, 171
 Pickett, B. K., Durisen, R. H., & Link, R. 1997, *Icarus*, 126, 243
 Pudritz, R. E., Banerjee, R., & Ouyed, R. 2008, *ArXiv e-prints*
 Różyczka, M., Bodenheimer, P., & Bell, K. R. 1994, *ApJ*, 423, 736
 Saigo, K., Tomisaka, K., & Matsumoto, T. 2008, *ApJ*, 674, 997
 Scott, E. R. D. 2007, *Ann. Rev. Earth Planet. Sci.*, 35, 577
 Stamatellos, D., Whitworth, A. P., Bisbas, T., & Goodwin, S. 2007, *A&A*, 475, 37
 Terebey, S., Shu, F. H., & Cassen, P. 1984, *ApJ*, 286, 529
 Thrane, K., Bizzarro, M., & Baker, J. A. 2006, *ApJ*, 646, L159
 Tohline, J. E. 2002, *ARA&A*, 40, 349
 Toman, J., Imamura, J. N., & Pickett, B. K. 1998, *ApJ*, 497, 370
 Tscharnuter, W. M. 1987, *A&A*, 188, 55
 Wuchterl, G., & Tscharnuter, W. M. 2003, *A&A*, 398, 1081
 Yorke, H. W., Bodenheimer, P., & Laughlin, G. 1993, *ApJ*, 411, 274
 Young, E. D., Simon, J. I., Galy, A., et al. 2005, *Science*, 308, 223